PRIMARY RESEARCH ARTICLE

Global Change Biology WILEY

Aged soils contribute little to contemporary carbon cycling downstream of thawing permafrost peatlands

Andrew J. Tanentzap[1] | Katheryn Burd[2] | McKenzie Kuhn[2] |
Cristian Estop-Aragonés[2] | Suzanne E. Tank[3] | David Olefeldt[2]

[1]Ecosystems and Global Change Group, Department of Plant Sciences, University of Cambridge, Cambridge, UK

[2]Department of Renewable Resources, University of Alberta, Edmonton, AB, Canada

[3]Department of Biological Sciences, University of Alberta, Edmonton, AB, Canada

Correspondence
Andrew J. Tanentzap, Ecosystems and Global Change Group, Department of Plant Sciences, University of Cambridge, Cambridge, CB2 3EA, UK.
Email: ajt65@cam.ac.uk

Present address
Cristian Estop-Aragonés, Ecohydrology and Biogeochemistry Group, Institute of Landscape Ecology, University of Münster, Münster, Germany

Abstract

Vast stores of millennial-aged soil carbon (MSC) in permafrost peatlands risk leaching into the contemporary carbon cycle after thaw caused by climate warming or increased wildfire activity. Here we tracked the export and downstream fate of MSC from two peatland-dominated catchments in subarctic Canada, one of which was recently affected by wildlife. We tested whether thermokarst bog expansion and deepening of seasonally thawed soils due to wildfire increased the contributions of MSC to downstream waters. Despite being available for lateral transport, MSC accounted for ≤6% of dissolved organic carbon (DOC) pools at catchment outlets. Assimilation of MSC into the aquatic food web could not explain its absence at the outlets. Using $\delta^{13}C$-$\Delta^{14}C$-$\delta^{15}N$-δ^2H measurements, we estimated only 7% of consumer biomass came from MSC by direct assimilation and algal recycling of heterotrophic respiration. Recent wildfire that caused seasonally thawed soils to reach twice as deep in one catchment did not change these results. In contrast to many other Arctic ecosystems undergoing climate warming, we suggest waterlogged peatlands will protect against downstream delivery and transformation of MSC after climate- and wildfire-induced permafrost thaw.

KEYWORDS
boreal, carbon cycling, disturbance, food webs, permafrost peatlands, streams, terrestrial–aquatic linkages

1 | INTRODUCTION

Thawing of perennially frozen ground (i.e. permafrost) risks mobilizing vast stocks of aged carbon (C) downstream where they can be incorporated into the contemporary aquatic C cycle. These stocks are greatest in the thick (>1 m) organic layers of boreal peatlands affected by permafrost. Frozen and waterlogged conditions in these sites have slowed microbial decomposition and allowed about 180 Pg C, or one-fifth of all C in the atmosphere, to accumulate over centuries and millennia (Hugelius et al., 2020; Olefeldt et al., 2016). If centennial- to millennial-aged stocks, hereafter termed 'old' C, are subsequently exported and used downstream by aquatic food webs, they may amplify the positive feedback to climate warming caused by thawing soils respiring C faster than it is fixed on land (Schuur et al., 2015).

Both accelerated climate warming and wildfire activity are causing widespread permafrost thaw in boreal peatlands (Gibson et al.,

2018; Hugelius et al., 2020), but virtually nothing is known about whether these disturbances will also increase the amount of old soil C mobilized into aquatic ecosystems (Estop-Aragonés et al., 2020). The hydrology of boreal peatlands, where water moves from permafrost plateaus into permafrost-free bogs and fens (Connon et al., 2014), makes the transport of soil C unique. Excess ground ice that elevates peat plateaus above surrounding non-permafrost bogs and fens by about 1–3 m favours lateral flow paths (Quinton et al., 2019; Wright et al., 2009), which keep plateaus relatively dry and oxic, enabling open forests to develop (Quinton & Baltzer, 2013). As the seasonally thawed ground above permafrost (i.e. active layer) becomes thicker from climate warming and wildfire (Gibson et al., 2018; Quinton & Baltzer, 2013), more and older soil is exposed to leaching and microbial processing. Flow paths can then move through these layers and export old dissolved organic carbon (DOC; Frey & McClelland, 2009; Neff et al., 2006; Vonk et al., 2015). By contrast, when the entire soil profile thaws, peat plateaus collapse and become flooded in a process known as thermokarst, eventually expanding existing bogs and fens (Connon et al., 2014, 2015). Bogs and fens formed after thermokarst laterally export more recently fixed DOC than intact permafrost peat plateaus because of their more productive moss vegetation (Burd et al., 2020; Camill et al., 2001; Turetsky et al., 2007). The higher water table and anoxia in thermokarst bogs and fens also protects older C stocks deep in the soil profile from microbial processing (Campeau et al., 2019; Lee et al., 2012; Wilson et al., 2016).

Resource use by aquatic biota can provide additional evidence of whether old soil C is incorporated into the contemporary C cycle. Old C can be assimilated by secondary consumers directly or by ingesting microbes that metabolized these sources (Bellamy & Bauer, 2017). For example, O'Donnell et al. (2020) found macroinvertebrates and fish had radiocarbon ages of up to several thousand years across 12 streams draining boreal to tundra landscapes, including from Yedoma areas where DOC may be particularly labile (Drake et al., 2015). Higher trophic levels can also appear aged if old C respired by microbes is fixed by photosynthetic organisms at the base of the food web (Guillemette et al., 2017). For these reasons, secondary consumers provide an integrated perspective on the fate of old soil C in aquatic ecosystems. Few studies, however, have directly related the use of old C by secondary consumers to permafrost thaw. In many boreal peatlands, organic matter was present in soils for centuries to millennia before permafrost formed (Heffernan et al., 2020; Pelletier et al., 2017). Consequently, the remaining old C may be highly recalcitrant (Burd et al., 2020) and poorly assimilated into downstream food webs after permafrost thaw.

Here we assessed how thawing peatland soils contributed to downstream aquatic C cycling after catchment disturbance in the discontinuous permafrost zone of the Northwest Territories, Canada. We first used radiocarbon to date DOC in laterally mobile, shallow groundwater of permafrost peat plateaus that were undisturbed or burned by wildfire 4 years prior, and in a thermokarst bog formed by permafrost thaw about 100 years ago (Pelletier et al., 2017; Figure 1a). We expected thermokarst bogs would have more modern DOC in shallow groundwater than undisturbed peat plateaus if their higher water table routed flow paths through recent

and more productive *Sphagnum* vegetation and maintained anaerobic conditions that protected deeper C stocks from being degraded into soluble compounds. By contrast, we expected relatively older DOC in shallow groundwater of burned peat plateaus due to their deeper active layer with predominantly oxic conditions. Measured active layer depths were twice as deep in the burned plateaus than in unburned plateaus by the end of the growing season in the year prior to our study: 118 and 58 cm, respectively (Gibson et al., 2018). We then estimated the contribution of different C sources to DOC collected in streams draining a burned and unburned catchment using two age attribution models (Raymond et al., 2007; Wild et al., 2019). The two catchments had similar land cover—nearly 50% permafrost peat plateaus and thermokarst bogs (Burd et al., 2018)—differing primarily in active layer depths of the plateaus (Gibson et al., 2018). We therefore tested whether DOC in outlets of burned catchments would appear older and more so as the summer progressed and the frost table deepened into the soil profile. Finally, we tested whether permafrost thaw mobilized old soil C into the biomass of contemporary aquatic consumers. Our food web sampling coincided with late-summer months, when we expected active layers to be fully thawed and thus DOC from old soils to be most available for transport and assimilation into the downstream C cycle.

2 | METHODS

2.1 | Study sites

We studied two catchments drained by Scotty Creek (61°18′N, 121°18′W) and Notawohka Creek (61°8′N, 120°17′W) in the discontinuous permafrost zone of the western Canadian boreal forest. The catchments were in close proximity (c. 50 km) and with comparable size (Scotty: 134 km^2; Notawohka: 321 km^2), geology (carbonate-based bedrock overtopped by glacial deposits), topography (flat to gently sloping), climate (including total runoff in recent years), and land cover (Burd et al., 2018). Nearly half of each catchment was covered by peatland complexes comprised of permafrost peat plateaus dominated by black spruce (*Picea mariana*) and permafrost-free thermokarst bogs dominated by *Sphagnum* spp. mosses. Remaining land cover was mostly upland mixed-wood forest characterized by trembling aspen (*Populus tremuloides*) and white spruce (*Picea glauca*). Despite the similarity in almost all respects, >90% of Notawohka was burned in 2013 while Scotty has been unaffected by any major fire in the last 60 years. We thus referred to the sites as the burned and unburned catchments, respectively. At each site, we focused our sampling at outlets accessible by road with comparable stream depth (c. 0.5–1.5 m) and width (<10 m).

2.2 | Water sampling

We measured radiocarbon ages of DOC in peatland shallow groundwater and stream outlets. We collected shallow groundwater
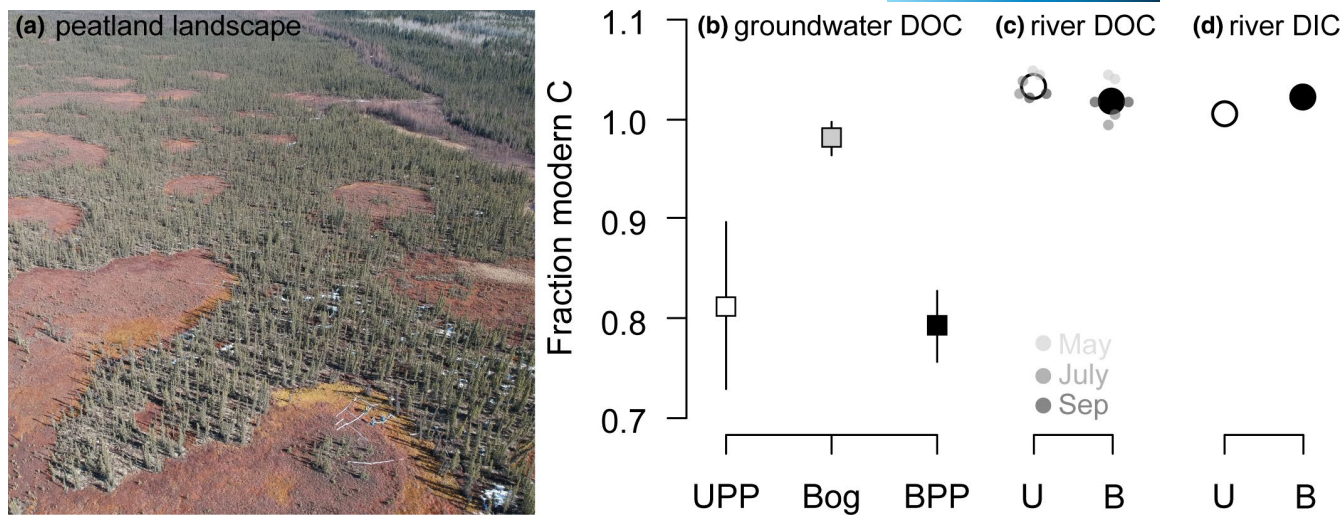
FIGURE 1 Fluvial carbon is relatively modern despite draining old peatland soils. (a) Aerial image of study landscape showing treed peat plateaus adjacent to *Sphagnum*-dominated thermokarst bogs. We measured the fraction of modern C defined as AD 1950 in DOC of (b) shallow groundwater from unburned (U) and burned (B) permafrost peatlands (PP) and a thermokarst bog (*n* = 3 per site in September) and (c) outlets draining U and B catchments (*n* = 6 per site evenly split across three dates). We concurrently measured (d) outlet DIC in September (*n* = 2 per site). Symbols are means ± standard errors. In (c) and (d), errors are indistinguishable. The fraction of modern C in atmospheric CO_2 during sampling was estimated to be 1.035

upstream of catchment outlets in September 2017 from a thermokarst bog and both burned and unburned peat plateaus. In each peatland, we dug pits to the top of the water table (depth for bog: 7–28 cm; burned peat: 24–42 cm; unburned peat: 24–34 cm), which has been shown to be laterally mobile and hydrologically connected with catchment outlets at one of our study sites (Quinton et al., 2019). We then inserted ten 12 cm long MacroRhizons (0.15 µm pore size; Rhizosphere Research Products) vertically into the soil with the other end connected to 60 ml syringes. The MacroRhizons are non-destructive, inert samplers that effectively capture dissolved components in soils (Seeberg-Elverfeldt et al., 2005). At each peatland, we filled pre-combusted glass bottles (0.5 L) in triplicate with shallow groundwater from at least one soil pit (total *n* = 9). Water was filtered in the field through pre-baked 0.7 µm glass fibre filters (475℃ for 4 h) using a pre-baked glass filtration assembly (500℃ for 4 h). Samples were stored in the dark and cold to minimize degradation of DOC.

We also collected two 2 L surface grab samples from each catchment outlet once in May, July, and September of 2017 (total *n* = 12). Samples were filtered and stored like those from groundwaters. $DO^{14}C$ was determined on all samples and $DI^{14}C$ was measured for September water only. Concurrently, we measured DOC concentrations 12 times in each outlet from May to October 2017. Samples were filtered as for radiocarbon, and then acidified with 0.6 ml 2 N HCl to pH < 2 before being analysed on a Shimadzu TOC-L within 8 days of collection (Shimadzu Co).

2.3 | Food web sampling

We sampled the aquatic food web in each of the two streams during September 2017 for isotopic composition ($\delta^{13}C$-$\Delta^{14}C$-$\delta^{15}N$-δ^2H). For

the consumers, we collected invertebrates by repeatedly sweeping across each outlet with a 500 µm mesh D-frame kicknet. Individuals were sorted in the field to Order level, either Amphipoda (crustacean amphipods) or larval insects in the Ephemeroptera (mayflies) and Odonata (dragonflies). After washing individuals into vials with Milli-Q water, they were left for c. 2 h to allow for digestion, assimilation, and/or gut evacuation (Persaud et al., 2009). We pooled c. 40 Amphipoda, 15 Ephemeroptera, and 3 Odonata per vial to have enough mass for three different isotopic analyses (see below). In total, we had *n* = 3 Amphipoda and *n* = 2 Ephemeroptera samples (all from the burned site) and *n* = 2 Odonata samples from each site. We also collected ninespine stickleback (*Pungitius pungitius*, *n* = 10) and young-of-the-year creek chub (*Semotilus atromaculatus*, *n* = 9 all at the unburned site) using the kicknet. Again, whole individuals were pooled in groups of 2–3 based on similar body length to have enough mass for isotope analyses (total *n* = 7). All samples were flash frozen on dry ice.

We also collected three autochthonous and allochthonous basal resources available to consumers in each site to measure their isotopic composition ($\delta^{13}C$-$\Delta^{14}C$-$\delta^{15}N$-δ^2H). First, we isolated phytoplankton clumps from the sweep netting and epilithic algae that were scraped from hard surfaces (*n* = 3 per site). Second, we collected leaf litter of the dominant terrestrial plants from the soil surface in each of the mixed-wood forest, thermokarst bog, and burned and unburned peat plateaus (*n* = 3 samples per site). Finally, we characterized old soil organic matter with two cores from a permafrost peat plateau within the unburned catchment. The first core (SC1) was collected in July 2013 with a 10 cm coring auger and 1 cm sections at nine depths from 35 to 326 cm were analysed for $\Delta^{14}C$ by Pelletier et al. (2017). The second core (MT8) was collected less than 500 m away in the same catchment in August 2014 using the same

methods (Pelletier et al., 2017), before being placed in a capped PVC tube and immediately frozen using dry ice. The core was sectioned into 1 cm slices in the laboratory and stored at −20℃. To characterize $\delta^{13}C$, $\delta^{15}N$, and δ^2H of soil organic matter near the bottom of the active layer, we dissected *Sphagnum* fragments from the MT8 core in the laboratory. Fragments were taken at depths of 50–51, 55–56, and 59–60 cm to characterize unburned sites and 130–131, 135–136, and 139–140 cm to characterize burned sites. Material was rinsed in Milli-Q water to remove any contaminants. All consumer and resource samples were oven-dried at 50℃ and ground into a homogeneous mixture.

2.4 | Isotope measurements

All samples were analysed for radiocarbon on a 3 MV tandem accelerator mass spectrometer at the A.E. Lalonde AMS Laboratory, University of Ottawa as described in Crann et al. (2017). The fraction of modern carbon, $F^{14}C$, was calculated as the ratio of $^{14}C/^{12}C$ in sample to a simultaneously measured oxalic acid II standard (Reimer et al., 2004), with all appropriate background and machine corrections (Crann et al., 2017). Values were converted to radiocarbon ages (uncalibrated) in years before present (i.e. 1950) as $-8033\ln(F^{14}C)$ and age-corrected isotope ratios $\Delta^{14}C$ as $(F^{14}C \times e^{[(1950 - y)/8267]} - 1) \times 1000$, where y was the measurement year. We used CALIBomb (http://calib.qub.ac.uk/CALIBomb/) to estimate any calendar ages ±1σ with standard calibration datasets (Hua et al., 2013; Reimer et al., 2013). As $\Delta^{14}C$ data already existed for one of the two soil cores (SC1), we did not analyse the second core (MT8) for radiocarbon. Instead, we estimated ages of 1 cm sections from an age-depth model fitted to existing data for the SC1 core from Pelletier et al. (2017). We estimated the age-depth model with a Bayesian accumulation history fitted by the *rbacon* package in R v.3.5 and extracted a posterior mean and standard deviation for the age of each depth interval (Blaauw & Christen, 2011). Values were converted to $\Delta^{14}C$ to be comparable with measurements of DOC and aquatic consumers by interpolating between the nearest uncalibrated radiocarbon ages from Reimer et al. (2013).

We also measured all samples for stable isotopes at the G.G. Hatch Laboratory, University of Ottawa. Ratios of both $\delta^{13}C$ and $\delta^{15}N$ and separately δ^2H were measured on isotope-ratio mass spectrometers calibrated with international standards (Brodie et al., 2011). We also measured the September outlet water samples for δ^2H ratios on an isotope water analyser at the G.G. Hatch Laboratory (Berman et al., 2013) to correct consumer resource use for dietary water uptake (see below). Finally, we confirmed that H-exchange was negligible with an experiment modelled after Bowen et al. (2005) for each sample type (mean fraction of exchangeable hydrogen ±1 SD: 0.032 ± 0.25). Importantly, removing δ^2H from the mixing model made no difference to our conclusions (Spearman's rank correlation ρ = 0.99 between resource use for consumer model described below estimated with and without δ^2H; Figure S1).

2.5 | Statistical analyses of dissolved carbon

We tested whether active layer deepening changed the mean age of shallow groundwater and stream-water C using linear models. We compared log-transformed radiocarbon ages of shallow groundwater $DO^{14}C$ in the thermokarst bog and burned peat plateau to ages in the unburned peat plateau. Peatland type was the only predictor variable. We also compared outlet DOC between the two catchments, accounting for random variation among sampling months in each catchment and using $F^{14}C$ rather than age as the response. Radiocarbon age could not be analytically solved in the outlets because all but two $F^{14}C$ values were >1.1, suggesting they comprised material since nuclear weapons testing of the late 1950s to early 1960s and for which a unique age could not be assigned (Reimer et al., 2004). Finally, we used a paired t test to compare DOC concentration between catchment outlets as samples were taken within 2 days of each other throughout the year. All analyses were performed in R v.3.5 with Stan v.2.17 used for statistical modelling (see Methods S1 for full details of model fitting). R code to reproduce the analyses is given in Data S1 and available with the corresponding data at https://github.com/atanzap/agedcarbon.

We also modelled the age distribution of DOC in each shallow groundwater type and tested whether it varied between the outlets of unburned and burned catchments. Although a single mean age of DOC is estimated by radiocarbon dating, DOC is actually a mixture of compounds of varying age (Dean et al., 2019). To estimate the contribution made by older groundwater to this mixture, we used a simple age attribution model that relates DOC production to age in vertical peat profiles (Dean et al., 2018; Evans et al., 2014; Raymond et al., 2007). This approach assumes that DOC in shallow groundwater is dominated by primary production in the year prior to sampling and proportional contributions from past years decline exponentially with time at a constant rate k (year^{-1}). Comparing k between catchments therefore allowed us to test whether wildfire changed the rate at which old peat contributed to DOC pools available for hydrological export. Conceptually, the model is consistent with empirical observations of decomposition and hydrology downwards through peat profiles (Hoag & Price, 1995; Holden & Burt, 2003; Limpens et al., 2008). We then estimated k for each groundwater type and catchment by modelling the mean $F^{14}C$ of DOC from $F^{14}C$ reconstructed for atmospheric $^{14}CO_2$ (A_t) for each year t over the past 10,000 years, which we assumed was equal to ^{14}C in peat organic matter accumulated during that year (Moore et al., 2013):

$$F^{14}C = \sum_{t=1}^{t=10,000} \left(e^{-k(t-1)} - e^{-kt}\right) A_t. \tag{1}$$

Atmospheric $^{14}CO_2$ was derived using Reimer et al. (2013) for pre-1950 values, annual means of Hua et al. (2013) for 1950–2010, and a spline fitted to the two datasets using the *smooth.spline* function in R to extrapolate post-2010 values.

Finally, we quantified how much old soil C contributed to DOC in the catchment outlets using the isotope-based source apportionment

model of Wild et al. (2019). Fluvial DOC in permafrost peatlands is primarily derived from gradual leaching of recent terrestrial primary production at the soil surface, with smaller contributions from soils deeper in the active layer (Wild et al., 2019). Therefore, following Wild et al. (2019), we assumed that $\Delta^{14}C$ ratios of DOC in each outlet were normally distributed with a mean determined by a mixture of DOC from shallow groundwater of peat plateaus P and leached from surficial litterfall R. The proportional contribution p to each observation i of outlet $\Delta^{14}C$ from the mean $\Delta^{14}C$ of each source could then be estimated in each catchment j in each month t as:

$$\Delta^{14}C_{ijt} = p_{jt}P_j + (1 - p_{jt})R_j, \qquad (2)$$

and we propagated the uncertainty in each source into the estimated SD of outlet DOC. P_j was characterized by groundwater $\Delta^{14}C$ at the top of the water table separately measured in unburned and burned peat plateaus. We also considered that DOC could be leached from soils at the bottom of the active layer in each peat plateau, and refit the model with P_j characterized by $\Delta^{14}C$ estimated at the bottom of the active layer from the age-depth model fitted to the dated peat core. We let active layer depth vary among months from 26 and 31 cm in June to 58 and 118 cm in September based on the most likely values in the unburned and burned catchments, respectively, measured by Gibson et al. (2018). Together, our two P_j scenarios represented the upper limit for the contribution of old soil C to fluvial DOC because we excluded any possible contribution from deeper frozen layers, as might arise from abrupt ground collapse (Wild et al., 2019). R_j was constrained from litterfall measured in peat plateaus and thermokarst bogs. To allow contributions from soil C to vary with the deeper active layers arising from wildfire w_j, and be constrained between 0 and 1, we modelled mean p_{jt} from a Beta distribution as:

$$\text{logit}(p_{jt}) = \alpha + \beta w_j + \upsilon_t, \qquad (3)$$

where α was an estimated mean, β was the effect of wildfire, and υ_t accounted for random variation among months and was estimated from a zero-mean normal distribution with separately estimated SD.

2.6 | Statistical analysis of resource use by aquatic consumers

We estimated how much old organic matter was utilized by the aquatic food web with a four-isotope ($\delta^{13}C$-$\Delta^{14}C$-$\delta^{15}N$-δ^2H) mixing model. We have previously found this model to recover known parameters with relatively high precision and accuracy, that is, <10% relative bias (Tanentzap et al., 2017). Briefly, the model estimated the proportion of different resources used by crustacean amphipods, aquatic insects, or fish from isotopic ratios observed in their body tissues and the mean and SD of isotopic ratios in modern plant litter, shallow groundwater DOC from peat plateaus, and epilithic algae. The functional form of this model resembled Equation (2), but with more potential resources and isotopes (see Methods S1 for full

notation). For modern plant litter, we weighted isotope ratios by the proportion of land cover occupied by wetland (i.e. both thermokarst bogs and permafrost peatlands) and upland forest in each catchment (Burd et al., 2018). For shallow groundwaters, we used $\delta^{13}C$, $\delta^{15}N$, and δ^2H observed in solid peat beneath the top of the water table, that is, 50–60 cm depth. However, we assumed isotopic ratios of DOC leached from peat throughout the saturated layer would be consistent with those at the top of the water table because they are preserved by waterlogged conditions that slow decomposition (Krüger et al., 2014). This assumption was partly supported by the lack of correlation between depth and either $\delta^{13}C$ or $\delta^{15}N$ when fitting a linear model to measurements across the 50–130 cm depth range ($t_4 = 1.56$, $p = 0.194$ and $t_4 = -2.69$, $p = 0.055$, respectively). There was a statistically significant change in δ^2H ($t_4 = -3.76$, $p = 0.020$), but this effect was negligible (mean ± SD: $0.06 \pm 0.02\%$ cm^{-1} of mean δ^2H). Nonetheless, the model accounted for potential fractionation effects, such as from preferential decomposition of lighter isotopes in deeper layers, by incorporating uncertainty in the isotopic ratios of resources. Finally, the model also accounted for physiological differences of biota by estimating a unique trophic position, trophic-level fractionation of $\delta^{15}N$, and contribution of dietary water to δ^2H ratios for each consumer from published information (Methods S1). Lipid correction was not applied to consumers as it was likely inappropriate in our case, i.e. when estimating dietary proportions from whole-body isotopic signatures (Arostegui et al., 2019), and it made no difference to our results (Figure S2).

In addition to the shallow groundwater model, we also tested whether solid peat from the bottom of the active layer directly contributed DOC or POC to consumer biomass. Using the age-depth model for the dated peat core (SC1), we estimated $\Delta^{14}C$ for active layer depths in the unburned and burned catchments at the time of food web sampling (58 and 118 cm, respectively; Gibson et al., 2018). For $\delta^{13}C$, $\delta^{15}N$, and δ^2H, we took the nearest solid peat measurements at 50–60 and 130–140 cm deep from the MT8 soil core for the unburned and burned catchments, respectively. As peat tends to be highly depleted in $\Delta^{14}C$ relative to DOC (Chasar et al., 2000), separate models with shallow groundwater DOC versus peat at the bottom of the active layer can be considered to represent the 'youngest' (i.e. maximum) and 'oldest' (i.e. minimum) contributions of peatland soils to the aquatic food web, respectively (after Wild et al., 2019).

We also tested whether consumers used resources differently between the burned and unburned catchments. To do so, we estimated the proportional contribution of old organic matter from old soils $p_{o,ijl}$ to each observation i of consumer l in catchment j from a Beta distribution with an estimated mean o_{jl} and SD:

$$\text{logit}(o_{jl}) = \alpha + \beta w_j + \upsilon_l, \qquad (4)$$

where α and β were as in Equation (3) and υ_l accounted for random variation with repeated observations of the same consumer and was sampled from a zero-mean normal distribution with estimated SD. As total resource use had to sum to one, mean contributions from

modern plant litter $p_{f,ijl}$ and algae $p_{a,ijl}$ were equal to $(1 - p_{o,ijl})$, and we could also estimate the mean of $p_{a,ijl}$ by refitting Equation (4) as logit$^{-1}(\alpha + \beta w_j + v_l) \times (1 - p_{o,ijl})$. The simplex constraint then reduced $p_{f,ijl}$ to equal $1 - p_{o,ijl} - p_{a,ijl}$.

2.7 | Statistical analysis of resource use by aquatic primary producers

To determine whether DIC was aging the aquatic food web, we fitted the consumer isotopic mixing model to observations of $\delta^{13}C$ and $\Delta^{14}C$ in epilithic algae. DIC primarily comes from mineralization of terrestrial organic matter, geological weathering, and atmospheric CO_2 exchange (Campeau et al., 2017). We further distinguished terrestrial sources between soils from the organic horizon, measured by litterfall, and the active layer, measured by shallow groundwater DOC, and used their corresponding isotope ratios in our model. Once CO_2 from heterotrophic activity is dissolved in soils, its $\delta^{13}C$ values also become enriched by 1–4‰ because of selective gas exchange through soil pores (Amiotte-Suchet et al., 1999). We therefore let $\delta^{13}CO_2$ of our three sources be enriched by a median of 2.5‰ as they moved from soils into streams. We also refitted this model using solid peat at the bottom of the active layer as a terrestrial DIC source instead of shallow groundwater DOC. Peatland soils can also export large quantities of CH_4 to fluvial networks, especially from anaerobic conditions in the active layer (Campeau et al., 2014; Dinsmore et al., 2010; Olid et al., 2021 but see Street et al., 2016). This CH_4 can then be made available for autotrophic growth by methane-oxidizing bacteria (Grey, 2016; Kohzu et al., 2004; Raghoebarsing et al., 2005). We therefore considered CO_2 respired from methanotrophs as a fourth source of terrestrial DIC and set the corresponding $\delta^{13}CO_2$ to a mean ± SD of −50 ± 5‰ based on published data (Whiticar, 1999). This value was consistent with other food web studies (Kankaala et al., 2006) and equivalent to assuming the range of values in Nykänen et al. (2014) was roughly three times the SD. We let the $\Delta^{14}C$ ratio of this source equal that of shallow groundwater DOC as we assumed it was produced from the same source material, particularly at depth (Chanton et al., 2008), that is, the base of the active layer. We also had no reason to expect the $\Delta^{14}C$ ratio to change from methanogenesis followed by methanotrophy. Geological sources had a mean ± SD for $\delta^{13}C$ and $\Delta^{14}C$ of −1.25 ± 0.4‰ and −1000 ± 1.0‰, respectively (Whiticar, 1996). The $\Delta^{14}C$ estimate was consistent with the presumed age of glacial tills that characterize surface geology in our study region and were deposited during the glacial period (Aylsworth et al., 2000). For the atmospheric DIC source, we used our spline-estimated value of $\Delta^{14}C$ in 2017 (see above) and mean $\delta^{13}C$ from May to September 2017 at the Point Barrow, Alaska monitoring station (Keeling et al., 2005). We let the $\delta^{13}C$ value be enriched by 7‰ from diffusive exchange between the atmosphere and stream water (Wigley et al., 1978). Finally, we estimated fractionation of $\delta^{13}C$ by algae during photosynthesis (Bade et al., 2006).

We used a novel model averaging approach to combine estimates from the different isotopic mixing models fitted to the

epilithic algae. As we only measured two isotopes, a single model with all six potential DIC sources (surficial vegetation, shallow and deep active layer soils, methanotrophy, geological weathering, and atmospheric exchange) would have been statistically unidentifiable. We instead fitted separate models for each of the four terrestrial sources, all including geological and atmospheric sources. We then used bootstrapped-Pseudo-Bayesian model averaging (Pseudo-BMA+) to derive parameter estimates across the three models (Yao et al., 2018) with the *loo* package in R (Vehtari et al., 2017). This averaging approach was preferable because we wanted to calculate model weights separately. We expected some models to be more similar than others and did not want these to share weights through joint estimation, that is, stacking predictive distributions.

3 | RESULTS

3.1 | Low levels of old carbon recovered in catchment outlets

Old C stocks in shallow groundwater of the peat plateaus appeared little disturbed by active layer deepening after wildfire despite being available for lateral transport. DOC in shallow groundwater of permafrost peat plateaus during late summer was estimated to be between 568 and 3465 radiocarbon years old and was not older in the burned plateau, suggesting no major hydrological export of old C stocks after wildfire (t_6 = 0.37, p = 0.726; Figure 1b). The position of the water table supported this explanation. Despite a deeper thaw depth in the burned site, the water table was at similar depths between burned and unburned plateaus in late summer relative to a known marker in the soil profile, White River Ash tephra, which dates to c. 1260 year uncalibrated BP (Clague et al., 1995). Burned and unburned peatlands had mean (±standard deviation, SD) saturated zones that were 35 (±10) cm versus 27 (±6) cm beneath the soil surface, respectively, and 23 (±7) cm versus 18 (±6) cm beneath the White River Ash tephra. Thus, shallow groundwater must have received little DOC from deeper peat to not be more aged in the burned catchment, where soil thawed much deeper during late summer sampling.

DOC in shallow groundwater of the thermokarst bog also contained old soil C as it had a fraction of modern carbon ($F^{14}C$) beneath current atmospheric $^{14}CO_2$. Although this DOC was still, on average, younger than in the unburned permafrost peatland (t_6 = −3.24, p = 0.018; Figure 1b), DOC is a mixture of differently aged molecules. Large contributions from modern material can skew bulk age estimates and mask contributions from older sources, like deeper layers of peat plateaus. Upper soil profiles would have had elevated contributions to bulk DOC in the bog groundwater because of the higher water table (mean ± SD depth: 19 ± 2 cm; Wilcoxon–Mann–Whitney test for difference with unburned peatland: Z = −1.99, p = 0.046), and these have been disproportionately enriched in ^{14}C following aboveground nuclear testing of the 1950s and 1960s. A model of contributions towards DOC mixtures from different depths

in the peat profile supported this interpretation. We found that, despite these modern sources, 1000-year-old C was still present in bog groundwater, as expected whether the higher water table protected rather than destabilized old C captured from peat plateaus by lateral flow or thermokarst (Figure 2).

Despite old soil C being exposed to leaching and microbial processing by permafrost thaw, these stocks contributed little towards fluvial export of DOC from our study catchments. We found that DO^{14}C in catchment outlets during early summer exceeded modern values, indicating most of the C pool was recent and originated after enrichment of atmospheric $^{14}CO_2$ in the 1950s and 1960s (Figure 1c). Bulk DOC in catchment outlets did age during July and September when flow paths deepened relative to our initial May sampling (t_8 = −4.43, p = 0.002 and t_8 = −3.74, p = 0.006; respectively), but values were still younger than in shallow groundwater of the peat plateaus and bogs (Figure 1).

To disentangle the contributions of different aged C pools towards outlet DOC mixtures, we re-fitted the age-attribution model that assumed contributions of DOC from past years declined exponentially with time. This model estimated that 66% of DOC recovered at the catchment outlets was between 50 and 500 years old when averaged across summer observations, with 12% older than this range (Figure 3a,b). We then fitted a source attribution model to distinguish the contribution of different peatland sources towards outlet DO^{14}C. We assumed that outlet DOC was either recently fixed by surficial vegetation or came from shallow groundwater of peat plateau measured above, allowing this contribution to vary among months as hydrological connectivity changed. The Δ^{14}C values of recent terrestrial primary production were constrained with measurements of litter in peat plateaus and thermokarst bogs, all of which had modern radiocarbon ages, that is, post-1950. Using differences in Δ^{14}C signatures between potential sources, the model estimated that on average, across sites and sampling months, 9% (95% CI: 0% to 40%) of the outlet DOC came from shallow groundwater of peat plateaus (Figure 3c). Contributions were similar (mean:

7%; 95% CI: 0%–27%) when we let solid peat at the bottom of the active layer contribute to outlet DOC, with active layer depth varying among months as the soil thawed. At its deepest, the bottom of the active layer had solid peat with estimated mean ± SD ages of 1956 ± 265 and 2942 ± 843 radiocarbon years in the unburned and burned catchments, respectively.

Contributions of old soil C towards outlet DOC did not vary with active layer deepening in either age attribution model (Figure 3). In the first model, the rate at which DOC production declined with depth through the peat profile was indistinguishable between unburned and burned catchments despite active layers being nearly twice as deep in the latter (95% CI for effect of burning on decomposition rate k: −0.66 to 1.00). Similarly, peat plateaus contributed to outlet DOC similarly between catchments in the Δ^{14}C source attribution model either from shallow groundwater or solid peat at the bottom of the active layer (95% CI for effect of burning: −2.37 to 0.31 and −2.37 to 0.36 for each source, respectively). These results were consistent with observations of outlet DOC ages, which showed no average difference between catchments (95% CI: −0.12 to 0.10). Outlet DOC was only older in the burned catchment during July when low flow may have caused more water to be sourced from deeper soils (95% CI for difference in F^{14}C: 0.02 to 0.05). Although DOC concentrations were 1.6 mg L^{-1} higher, on average, in the burned than unburned outlet (mean ± standard error [SE] over the ice-free season: 20.7 ± 0.5 mg L^{-1} vs. 19.1 ± 0.5 mg L^{-1}, respectively; paired t_{11} = 2.29, p = 0.043), absolute DOC export was lower on an areal basis. We lacked corresponding estimates of total runoff during our measurements, but values differed by <10% between catchments in the previous year (Burd et al., 2018). Nonetheless, as the burned catchment had nearly three times the area of peat plateaus and thermokarst bogs (154 vs. 56 km^2 in the unburned site), it likely exported more old C on an absolute basis. Together, the two age attribution models suggested old C stocks were mostly stable despite thaw disturbance and/or were detected at low levels in outlet DOC pools because they were being preferentially consumed.
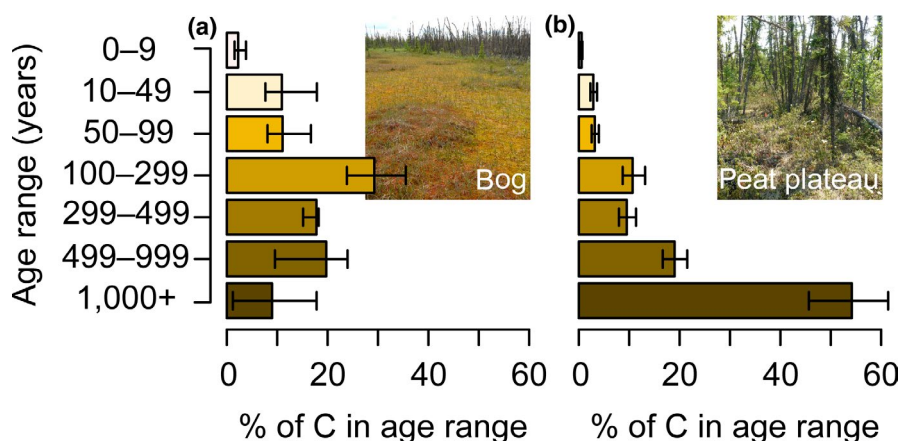

FIGURE 2 Shallow groundwater contains old carbon even after c. 100 years after thermokarst bog formation. Mean (±95% CI) percentage of carbon estimated in different age classes by assuming DOC production declines exponentially through vertical soil profiles of (a) a thermokarst bog and (b) burned and unburned permafrost peat plateaus. Peat plateaus were pooled for modelling after detecting no difference in age profiles (Figure 1)
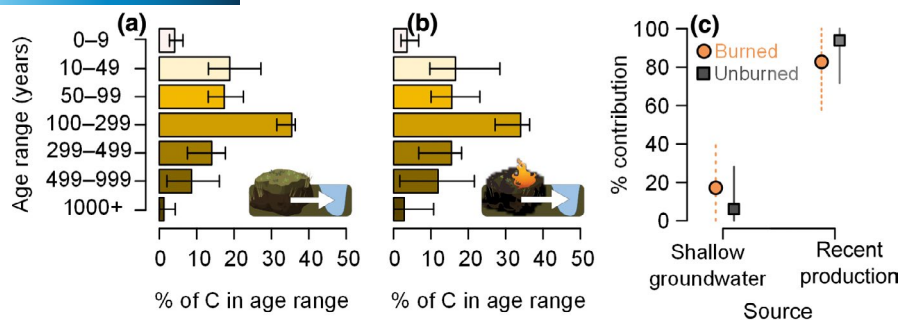
FIGURE 3 Old soil C from permafrost peatlands contributes relatively little to DOC in catchment outlets across summer. Mean (±95% CI) percentage of carbon in outlet DOC of (a) unburned and (b) burned catchments modelled by assuming DOC production declines exponentially through vertical peat profiles. White arrows scaled to mean DOC concentrations. We also estimated the (c) mean (±95% CI) percentage contribution to outlet DOC from shallow groundwater versus surficial vegetation of the peat plateau. We produced separate estimates in unburned and burned catchments with isotopic mixing models fitted to three sampling dates across summer 2017. Median R^2 = 0.90 for (a) and (b), 0.47 for (c)
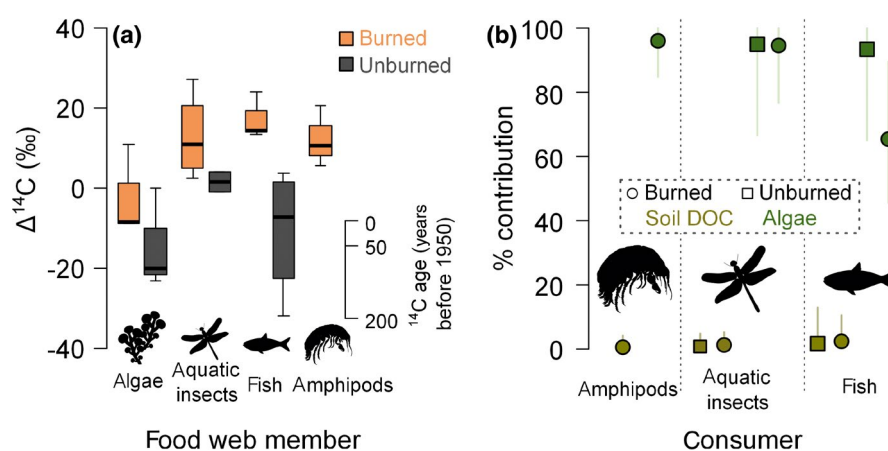

FIGURE 4 Low levels of old carbon in aquatic consumers at catchment outlets. (a) Boxplots of Δ^{14}C ratios and estimated radiocarbon ages of algae (n = 6) and aquatic consumers. We differentiated larval aquatic insects (Ephemeroptera and Odonata, n = 6), small fish (*Pungitius pungitius*, juvenile *Semotilus atromaculatus*; n = 7), and crustacean amphipods (Amphipoda; only present in burned catchment, n = 3) in burned and unburned catchments. (b) Mean percentage (±95% CI) of shallow groundwater DOC from peat plateaus and algal organic matter that contributed to consumer biomass. Estimates came from a four-isotope mixing model; see Table S1 for parameter estimates. Bayesian R^2 = 0.97 across isotopes

3.2 | Food web primarily assimilates modern terrestrial carbon

Dating of the aquatic food web discounted preferential assimilation of old C into biomass, despite consumers being visibly aged. To estimate the use of old soil C by aquatic consumers, we fitted a four-isotope (δ^{13}C-Δ^{14}C-δ^{15}N-δ^2H) mixing model that considered modern plant litter, DOC from peat plateau shallow groundwater, and epilithic algae as potential resources. While 2 of 7 young-of-the-year fish had radiocarbon ages of >40 years old (Figure 4a), peatland shallow groundwater DOC contributed only 0%–8% (95% CI) to biomass across consumers and sites (Figure 4b). This range overlapped with the amount of outlet DOC derived from peatland soils (Figure 3c). Thus, there was no difference between the contribution of old shallow groundwater DOC to catchment outlets versus consumer biomass when comparing posterior distributions of these estimates (95% CI of p values from Kolmogorov–Smirnov tests across 1000 samples: <0.001 to 0.364; Figure S3). The contribution to

consumer biomass was similar when shallow groundwater DOC was replaced as a food web resource with solid peat from the bottom of the active layer (95% CI: 0%–6%).

We found evidence that primary producers were fixing old DIC, thereby aging the aquatic food web, but little of this C came from the mineralization of soil organic matter. Across both sites, DIC was as aged as DOC (Wilcoxon signed-rank test, V = 7, p = 0.625; Figure 1), suggesting it contained similar amounts of old C (Figure 2). Epilithic algae, which most contributed to consumer biomass (95% CI: 53%–100%; Figure 4b), equally had pre-modern radiocarbon ages (Figure 4a). To link uptake of old C with biomass age at the base of the food web, we fitted another isotopic (δ^{13}C-Δ^{14}C) mixing model that apportioned C sources fixed by algae. This model separated contributions from atmospheric CO_2 and both biogenic (e.g. organic matter mineralization) and geogenic sources (Figure S4). We found that, averaged across sites, active layer soils contributed 3% (95% CI: 1%–5%) towards algal biomass from mineralization of either shallow groundwater DOC or solid peat into CO_2. Weathering contributed

slightly more by 1%–9% (95% CI), but mostly modern, surficial plant litter from the surrounding landscape accounted for much of the remainder (95% CI: 37%–69%; Figure 5; Figure S4).

Our algal δ^{13}C values were also among the most negative reported, to our knowledge (median δ^{13}C = −40‰; Figure S5), suggesting some DIC fixed by photosynthesis was highly depleted in δ^{13}C. CH_4 oxidation would produce the most depleted $^{13}CO_2$ in our system (mean δ^{13}C = −50‰). If the CH_4 came from anoxic layers at the bottom of the peatland active layer, it would have a similar Δ^{14}C as DOC and could simultaneously age algal biomass. Therefore, we tested whether algae used DIC produced by oxidation of CH_4 with Δ^{14}C identical to that of DOC in shallow groundwater and δ^{13}C = −50‰ (Figure S3), and found a small contribution (95% CI: 1%–4%). This model was better supported than one in which we let Δ^{14}C ratio of CH_4 equal present-day (i.e. atmospheric) values (pseudo-BMA + weights = 0.09 vs. 0.06, respectively, when included in the model set in Table S1). Overall, our models estimated that, on average, 6% (95% CI: 3%–13%) of consumer biomass came from old soil C when summing both the direct uptake of organic matter and indirect recycling of millennial-aged DIC via algal photosynthesis (Figure 5).

Old soil C was further excluded as an important resource in the aquatic food web by comparing the radiocarbon signature of biota between catchments. We specifically found that algae and consumers in the burned catchment had a higher mean Δ^{14}C (Figure 4a; t_{20} = 3.77, p = 0.001). As biota did not use resources differently between sites (Figure 4b; Table S1), this result was attributable to

differences in Δ^{14}C of peat plateau litter, which was the most used resource across the food web via both DIC and DOC (Figure 5). Litter left in the organic horizon of peat plateaus after wildfire was closer in Δ^{14}C to peak atmospheric values from aboveground nuclear testing, that is, more enriched (Figure S4). Estimated calendar ages indicated a 96% probability that the mean F^{14}C of peat plateau litter in the burned site was from 1991 to 2000, whereas all unburned litter was estimated to be post-2002.

4 | DISCUSSION

Here we found low levels of old C were released into the contemporary carbon cycle downstream of boreal peatlands after thermokarst bog formation or wildfire despite it being available for hydrological export in shallow groundwater. In all studies of smaller tributaries (i.e. creeks) draining undisturbed permafrost peatlands compiled by Estop-Aragonés et al. (2020), DOC was mostly modern, aside from a subset collected by O'Donnell et al. (2014). Gandois et al. (2019) similarly estimated that millennial-aged C from permafrost peatlands contributed <10% of DOC to a downstream lake. Our work advances our understanding of these dynamics by finding that DOC remains mostly modern even when these peatlands are disturbed by permafrost thaw associated with climate warming and wildfire. Likewise, future increases in DOC export after permafrost thaw (Frey & Smith, 2005; Olefeldt et al., 2014) may be primarily modern in origin. The scarcity of old soil C in downstream waters could not be explained by
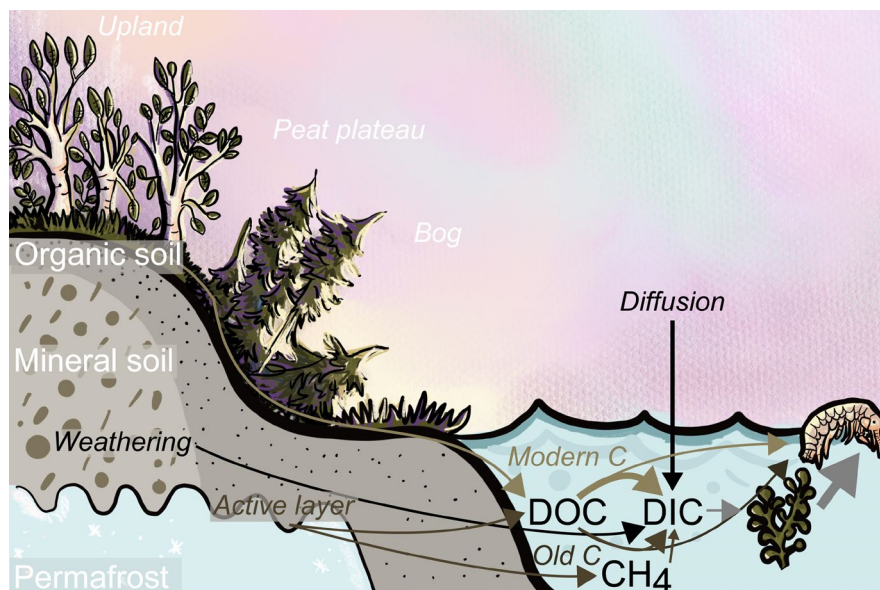

FIGURE 5 Flow of modern and old carbon from land into stream food webs through five potential pathways. We considered DIC fixed by algae could come from mineralization of modern surficial vegetation from peat plateaus, bogs, and upland forests; old soil C from the bottom of the active layer; oxidation of methane produced in anoxic layers of the active layer; weathering processes; or atmospheric diffusion. Consumers could assimilate algal C or DOC from either modern surficial vegetation or old soil C from the bottom of the active layer. Arrows are proportional to contributions towards algal and consumer biomass estimated from isotopic mixing models, with DIC pool used by algae in proportion to its availability. Colours group pathways into modern (light brown) and old (dark brown) soil C or weathering/atmospheric transfer (black). White text denotes different C sources

preferential mineralization, as porewater with old C sourced from the burned and unburned peat plateaus had relatively low biodegradability compared to younger DOC from the thermokarst bog (Burd et al., 2020). Using radiocarbon dating, we found the aquatic food web assimilated little old soil C. Instead, most of the biomass of aquatic consumers came from algal recycling of contemporary terrestrial C (Lennon et al., 2006). Thus, unlike regions where DOC released from thawing soils is old and highly labile (Abbott et al., 2014; Drake et al., 2015; Littlefair & Tank, 2018; Mann et al., 2015; Vonk et al., 2013), our work offers evidence that the vast old C stocks in boreal peatland soils appear protected from downstream export and food web assimilation after permafrost thaw. Alongside evidence from inland waters in tundra (Bouchard et al., 2015; Dean et al., 2020; Prėskienis et al., 2021) and more mineral- and ice-rich boreal catchments (Elder et al., 2019), we conclude that old C may not always be preferentially released and mineralized in downstream waters.

4.1 | Fluvial C export from boreal peatlands resilient to active layer deepening and thermokarst

Hydrological changes accompanying permafrost disturbance may protect old C in different ways between thermokarst bogs and peat plateaus. In thermokarst bogs, high water tables slow aerobic microbial activity and thus the mobilization of old C into downstream waters (Estop-Aragonés et al., 2020). Elevated CH_4 production in these environments (Olefeldt et al., 2013), which consists of some (<10%) previously frozen C from deeper soil horizons (Cooper et al., 2017), can also be accompanied by methane oxidation (Perryman et al., 2020). The greater productivity of vegetation in the bogs than the peat plateaus (Camill et al., 2001; Heffernan et al., 2020) could have also contributed more recent DOC to shallow groundwater and diluted aged signatures, especially if any exudates released at depth by woody plants on the plateaus were highly labile (Crow & Wieder, 2005). These processes would together explain the little old organic C and small amount of CH_4 from deeper soil layers that we estimated were exported into the aquatic food web. Thermokarst bogs may have also exported little old C because they remain hydrologically isolated in our landscape by surrounding permafrost peat plateaus that impede subsurface flow (Connon et al., 2014).

By contrast, limited subsurface flow from thawed peat plateaus rather than high water tables may have helped to protect old C after active layer deepening. As the frost table deepens during the growing season, the thawed saturated zone of peat plateaus moves into a zone of low hydraulic conductivity (Quinton & Baltzer, 2013). Lateral water movement correspondingly slows, and alongside typically drier conditions towards late summer, little old soil C may be mobilized laterally from peat plateaus. Although runoff is greater in spring, the shallower frost table, and thus flow paths, primarily exports younger soil C (Raymond et al., 2007), and we found that outlet DOC was youngest in May during the spring freshet. Stream DOC has also been found to become increasingly aged as the growing season progresses in other permafrost regions (Dean et al., 2018; Neff et al.,

2006). Evans et al. (2014) similarly found that water table depth was an overriding factor controlling fluvial export of old DOC from peatland soils. Degradation of old soil C into dissolved forms was mainly promoted by well-drained oxic soils (Evans et al., 2014). An additional explanation for our results is that peat plateaus route water to adjacent bogs and fens rather than directly to drainage outlets (Connon et al., 2014). As described above, the shallow water table, large storage capacity, and anaerobic conditions of these wetlands may slow and dilute the release of old C further downstream. Finally, the few bulk $DO^{14}C$ samples in our study may be unable to resolve small differences in the contributions of old soil C from active layer deepening (Wild et al., 2019). We estimated the true difference in contributions of old soil DOC between burned and unburned catchments in our source attribution model would be at most 5%–16% (95% CI) on an absolute basis so as not to detect significantly different posterior distributions given the observed bulk $DO\Delta^{14}C$ values.

4.2 | Aquatic food webs do not preferentially use old peatland C

The lack of preferential assimilation of old soil C into the aquatic food web contrasts with microbial communities elsewhere (Drake et al., 2015; Selvam et al., 2017) and may have arisen because of differences in permafrost formation. Most boreal peatlands are in the discontinuous permafrost zone (Hugelius et al., 2020), where thick peat layers and tall vegetation structures must form to facilitate downward freezing into soils (Shur & Jorgenson, 2007). Consequently, deeper and older peat is exposed to microbial activity for at least centuries to millennia before freezing, during which it can become relatively resistant to additional turnover (Heffernan et al., 2020; Pelletier et al., 2017). This process appears to make old peat less biodegradable should thawing occur (Burd et al., 2020; Leifeld et al., 2012; Pinsonneault et al., 2016) and limits its incorporation into higher trophic levels (O'Donnell et al., 2020). The higher mineral content of non-peatland soils can also sorb recalcitrant compounds that increase the bioavailability of old C (Kawahigashi et al., 2004; Littlefair & Tank, 2018). Although old peatland DOC can still be labile if permafrost aggraded after organic matter accumulation, such as in waterlogged soils that slow microbial degradation (Selvam et al., 2017), most peatlands in the discontinuous permafrost zone formed over drier ecosystems, that is, via paludification (Kuhry & Turunen, 2006), so our findings may be generalizable in this region.

Ecosystem properties rather than the structural composition of organic matter can also make compounds unavailable for microbial degradation and assimilation into the aquatic food web (Kothawala et al., 2021; Lehmann & Kleber, 2015). A study in Alaska found that the molecular composition of DOC exported along the permafrost–mineral interface was enriched in compounds indicative of microbial metabolism as compared with shallower flow paths through organic-rich horizons (Lynch et al., 2019). We may have therefore missed an important resource in our isotopic mixing models by considering only peat and not DOC at deeper depths, which can differ

in molecular composition (Chanton et al., 2008; MacDonald et al., 2021). However, our approach to use shallow groundwater DOC and peat at the base of the active layer as end members in our mixing model should encompass the range of potential isotopic composition available to downstream food webs. Concentrations of substrates unique to old DOC may have also been too dilute in our study relative to the microbial community (Kothawala et al., 2021; Lehmann et al., 2020). Consequently, these substrates would return a lower energetic return for microbes than the investment required for their assimilation and degradation (Kothawala et al., 2021; Lehmann et al., 2020). Even if only some of these substrates were unique to old versus active layer DOC, for example, 18% of the molecular formulas in polygonal peatlands studied by MacDonald et al. (2021), they would still help to limit the incorporation of old soil C into the downstream food web alongside the other mechanisms we have discussed.

4.3 | Wider implications for permafrost C cycling

The amount of old soil C lost through downstream transport may presently make little difference to C budgets in boreal peatland landscapes. In our sites, catchments can release between 1.5 and 2.8 g C m^{-2} of DOC in a year of average runoff (Burd et al., 2018). As our age distributions in stream outlets estimated a mean (95% CI) of 1.3% (0.04%–7.9%) of DOC was at least 1000 years old, then no more than 0.17 g C m^{-2} year^{-1} of millennial-aged soil C may leave the catchment as DOC. Relatedly, upwards of 0.63 (mean; 95% CI: 0.09–6.06) g C year^{-1} is estimated to be released as CO_2 per m^2 of watershed across fluvial networks of subarctic Canada (Hutchins et al., 2020). Assuming algae fix different CO_2 sources in proportion to their availability, our mixing models estimate that no more than 0.54 g C m^{-2} year^{-1} of the total CO_2 pool fixed by algae contains old soil C and is evaded from the stream network. These two fluxes summed are no more than 5% of the annual C accumulation in permafrost peatlands of c. 20 g C m^{-2} year^{-1} (Heffernan et al., 2020; Loisel et al., 2014). Moreover, assuming permafrost peat plateaus in our study region store at least 155 kg C m^{-2} (Heffernan et al., 2020), it would take millennia to deplete the millennial-aged soil C given these estimated rates. Although certainly preliminary, the magnitude of our calculations implies that permafrost peatlands are not amplifying climate warming by exporting old C into fluvial networks. Partly, active layer deepening may be causing old C to be respired before it is able to move laterally (Estop-Aragonés et al., 2018).

Because little old soil C is currently released into downstream waters, permafrost peatlands remain highly vulnerable to future disturbance. Specifically, the water table in permafrost-free bogs and fens can be permanently lowered by future warming that elevates both evapotranspiration (Helbig et al., 2020) and hydrological connectivity through loss of peat plateaus (Haynes et al., 2018). The lower water table will subsequently favour oxic conditions that enhance microbial decomposition (Alm et al., 1999; Ise et al., 2008; Olefeldt et al., 2017; Schädel et al., 2016), including of old soil C captured from peat plateaus (Estop-Aragonés et al., 2018). Similarly, reduced moisture deep

along the edges of collapsing peat plateaus could facilitate aerobic decomposition of old soil C (O'Donnell et al., 2012). Once dissolved or desorbed into soil water, old DOC may be transported downstream by lateral flow paths, which are further enhanced as wetlands become better connected to the drainage network with loss of permafrost (Haynes et al., 2018). Finally, catchment discharge can increase after permafrost thaw (Quinton et al., 2019), particularly during summer runoff (Burd et al., 2018), and remain elevated until most ground ice is lost (Gibson et al., 2019). More old soil C may therefore be exported after disturbances like wildfire without necessarily changing sources of DOC export (e.g. Granath et al., 2020). Although our results suggest less DOC export on an areal basis in the burned catchment with deeper active layers, future work that quantifies catchment carbon budgets over multiple seasons would help reduce uncertainty about the processes associated with the hydrological export of old soil C stocks. More generally, our work suggests that disturbances to local hydrology may threaten the future of old peatland C stocks more than the direct thawing of frozen organic matter.

ORCID

Andrew J. Tanentzap https://orcid.org/0000-0002-2883-1901
McKenzie Kuhn https://orcid.org/0000-0003-3871-1548
Cristian Estop-Aragonés https://orcid.org/0000-0003-3231-9967
Suzanne E. Tank https://orcid.org/0000-0002-5371-6577
David Olefeldt https://orcid.org/0000-0002-5976-1475

REFERENCES

Abbott, B. W., Larouche, J. R., Jones, J. B., Bowden, W. B., & Balser, A. W. (2014). Elevated dissolved organic carbon biodegradability from thawing and collapsing permafrost. *Journal of Geophysical Research: Biogeosciences*, *119*(10), 2049–2063. https://doi.org/10.1002/2014JG002678

Alm, J., Schulman, L., Walden, J., Nykänen, H., Martikainen, P. J., & Silvola, J. (1999). Carbon balance of a boreal bog during a year with an exceptionally dry summer. *Ecology*, *80*(1), 161–174.

Amiotte-Suchet, P., Aubert, D., Probst, J. L., Gauthier-Lafaye, F., Probst, A., Andreux, F., & Viville, D. (1999). δ13C pattern of dissolved

inorganic carbon in a small granitic catchment: The Strengbach case study (Vosges mountains, France). *Chemical Geology*, *159*(1), 129–145. https://doi.org/10.1016/S0009-2541(99)00037-6

Arostegui, M. C., Schindler, D. E., & Holtgrieve, G. W. (2019). Does lipid-correction introduce biases into isotopic mixing models? Implications for diet reconstruction studies. *Oecologia*, *191*(4), 745–755. https://doi.org/10.1007/s00442-019-04525-7

Aylsworth, J. M., Burgess, M. M., Desrochers, D. T., Duk-Rodkin, A., Robertson, T., & Traynor, J. A. (2000). Surficial geology, subsurface materials, and thaw sensitivity of sediments. In L. D. Dyke & G. R. Brooks (Eds.), *The physical environment of the Mackenzie Valley, Northwest Territories* (Vol. *547*, pp. 41–48). Natural Resources Canada. https://doi.org/10.4095/211911

Bade, D. L., Pace, M. L., Cole, J. J., & Carpenter, S. R. (2006). Can algal photosynthetic inorganic carbon isotope fractionation be predicted in lakes using existing models? *Aquatic Sciences*, *68*(2), 142–153. https://doi.org/10.1007/s00027-006-0818-5

Bellamy, A. R., & Bauer, J. E. (2017). Nutritional support of inland aquatic food webs by aged carbon and organic matter. *Limnology and Oceanography Letters*, *2*(5), 131–149. https://doi.org/10.1002/lol2.10044

Berman, E. S. F., Levin, N. E., Landais, A., Li, S., & Owano, T. (2013). Measurement of $\delta^{18}O$, $\delta^{17}O$, and ^{17}O-excess in water by off-axis integrated cavity output spectroscopy and isotope ratio mass spectrometry. *Analytical Chemistry*, *85*(21), 10392–10398. https://doi.org/10.1021/ac402366t

Blaauw, M., & Christen, J. A. (2011). Flexible paleoclimate age-depth models using an autoregressive gamma process. *Bayesian Analysis*, *6*(3), 457–474. https://doi.org/10.1214/11-BA618

Bouchard, F., Laurion, I., Prėskienis, V., Fortier, D., Xu, X., & Whiticar, M. J. (2015). Modern to millennium-old greenhouse gases emitted from ponds and lakes of the Eastern Canadian Arctic (Bylot Island, Nunavut). *Biogeosciences*, *12*(23), 7279–7298. https://doi.org/10.5194/bg-12-7279-2015

Bowen, G. J., Chesson, L., Nielson, K., Cerling, T. E., & Ehleringer, J. R. (2005). Treatment methods for the determination of δ^2H and $\delta^{18}O$ of hair keratin by continuous-flow isotope-ratio mass spectrometry. *Rapid Communications in Mass Spectrometry*, *19*(17), 2371–2378. https://doi.org/10.1002/rcm.2069

Brodie, C. R., Casford, J. S. L., Lloyd, J. M., Leng, M. J., Heaton, T. H. E., Kendrick, C. P., & Yongqiang, Z. (2011). Evidence for bias in C/N, $\delta^{13}C$ and $\delta^{15}N$ values of bulk organic matter, and on environmental interpretation, from a lake sedimentary sequence by pre-analysis acid treatment methods. *Quaternary Science Reviews*, *30*(21), 3076–3087. https://doi.org/10.1016/j.quascirev.2011.07.003

Burd, K., Estop-Aragonés, C., Tank, S. E., & Olefeldt, D. (2020). Lability of dissolved organic carbon from boreal peatlands: Interactions between permafrost thaw, wildfire, and season. *Canadian Journal of Soil Science*, *100*, 503–515. https://doi.org/10.1139/cjss-2019-0154

Burd, K., Tank, S. E., Dion, N., Quinton, W. L., Spence, C., Tanentzap, A. J., & Olefeldt, D. (2018). Seasonal shifts in export of DOC and nutrients from burned and unburned peatland-rich catchments, Northwest Territories, Canada. *Hydrology and Earth System Sciences*, *22*(8), 4455–4472. https://doi.org/10.5194/hess-22-4455-2018

Camill, P., Lynch, J. A., Clark, J. S., Adams, J. B., & Jordan, B. (2001). Changes in biomass, aboveground net primary production, and peat accumulation following permafrost thaw in the boreal peatlands of Manitoba, Canada. *Ecosystems*, *4*(5), 461–478. https://doi.org/10.1007/s10021-001-0022-3

Campeau, A., Bishop, K., Amvrosiadi, N., Billett, M. F., Garnett, M. H., Laudon, H., Öquist, M. G., & Wallin, M. B. (2019). Current forest carbon fixation fuels stream CO_2 emissions. *Nature Communications*, *10*(1), 1876. https://doi.org/10.1038/s41467-019-09922-3

Campeau, A., Lapierre, J.-F., Vachon, D., & del Giorgio, P. A. (2014). Regional contribution of CO_2 and CH_4 fluxes from the fluvial network in a lowland boreal landscape of Québec. *Global Biogeochemical Cycles*, *28*(1), 57–69. https://doi.org/10.1002/2013GB004685

Campeau, A., Wallin, M. B., Giesler, R., Löfgren, S., Mörth, C.-M., Schiff, S., Venkiteswaran, J. J., & Bishop, K. (2017). Multiple sources and sinks of dissolved inorganic carbon across Swedish streams, refocusing the lens of stable C isotopes. *Scientific Reports*, *7*(1), 9158. https://doi.org/10.1038/s41598-017-09049-9

Chanton, J. P., Glaser, P. H., Chasar, L. S., Burdige, D. J., Hines, M. E., Siegel, D. I., Tremblay, L. B., & Cooper, W. T. (2008). Radiocarbon evidence for the importance of surface vegetation on fermentation and methanogenesis in contrasting types of boreal peatlands. *Global Biogeochemical Cycles*, *22*(4). https://doi.org/10.1029/2008GB003274

Chasar, L. S., Chanton, J. P., Glaser, P. H., Siegel, D. I., & Rivers, J. S. (2000). Radiocarbon and stable carbon isotopic evidence for transport and transformation of dissolved organic carbon, dissolved inorganic carbon, and CH_4 in a northern Minnesota peatland. *Global Biogeochemical Cycles*, *14*(4), 1095–1108. https://doi.org/10.1029/1999GB001221

Clague, J. J., Evans, S. G., Rampton, V. N., & Woodsworth, G. J. (1995). Improved age estimates for the White River and Bridge River tephras, western Canada. *Canadian Journal of Earth Sciences*, *32*(8), 1172–1179. https://doi.org/10.1139/e95-096

Connon, R. F., Quinton, W. L., Craig, J. R., Hanisch, J., & Sonnentag, O. (2015). The hydrology of interconnected bog complexes in discontinuous permafrost terrains. *Hydrological Processes*, *29*(18), 3831–3847. https://doi.org/10.1002/hyp.10604

Connon, R. F., Quinton, W. L., Craig, J. R., & Hayashi, M. (2014). Changing hydrologic connectivity due to permafrost thaw in the lower Liard River valley, NWT, Canada. *Hydrological Processes*, *28*(14), 4163–4178. https://doi.org/10.1002/hyp.10206

Cooper, M. D. A., Estop-Aragonés, C., Fisher, J. P., Thierry, A., Garnett, M. H., Charman, D. J., Murton, J. B., Phoenix, G. K., Treharne, R., Kokelj, S. V., Wolfe, S. A., Lewkowicz, A. G., Williams, M., & Hartley, I. P. (2017). Limited contribution of permafrost carbon to methane release from thawing peatlands. *Nature Climate Change*, *7*(7), 507–511. https://doi.org/10.1038/nclimate3328

Crann, C. A., Murseli, S., St-Jean, G., Zhao, X., Clark, I. D., & Kieser, W. E. (2017). First status report on radiocarbon sample preparation techniques at the A.E. Lalonde AMS Laboratory (Ottawa, Canada). *Radiocarbon*, *59*(3), 695–704. https://doi.org/10.1017/RDC.2016.55

Crow, S. E., & Wieder, R. K. (2005). Sources of CO_2 emission from a northern peatland: root respiration, exudation, and decomposition. *Ecology*, *86*(7), 1825–1834. https://doi.org/10.1890/04-1575

Dean, J. F., Garnett, M. H., Spyrakos, E., & Billett, M. F. (2019). The potential hidden age of dissolved organic carbon exported by peatland streams. *Journal of Geophysical Research: Biogeosciences*, *124*(2), 328–341. https://doi.org/10.1029/2018JG004650

Dean, J. F., Meisel, O. H., Martyn Rosco, M., Marchesini, L. B., Garnett, M. H., Lenderink, H., van Logtestijn, R., Borges, A. V., Bouillon, S., Lambert, T., Röckmann, T., Maximov, T., Petrov, R., Karsanaev, S., Aerts, R., van Huissteden, J., Vonk, J. E., & Dolman, A. J. (2020). East Siberian Arctic inland waters emit mostly contemporary carbon. *Nature Communications*, *11*(1), 1627. https://doi.org/10.1038/s41467-020-15511-6

Dean, J. F., van der Velde, Y., Garnett, M. H., Dinsmore, K. J., Baxter, R., Lessels, J. S., Smith, P., Street, L. E., Subke, J.-A., Tetzlaff, D., Washbourne, I., Wookey, P. A., & Billett, M. F. (2018). Abundant pre-industrial carbon detected in Canadian Arctic headwaters: Implications for the permafrost carbon feedback. *Environmental Research Letters*, *13*(3), 034024. https://doi.org/10.1088/1748-9326/aaa1fe

Dinsmore, K. J., Billett, M. F., Skiba, U. M., Rees, R. M., Drewer, J., & Helfter, C. (2010). Role of the aquatic pathway in the carbon and greenhouse gas budgets of a peatland catchment. *Global Change Biology*, *16*(10), 2750–2762. https://doi.org/10.1111/j.1365-2486.2009.02119.x

Drake, T. W., Wickland, K. P., Spencer, R. G. M., McKnight, D. M., & Striegl, R. G. (2015). Ancient low–molecular-weight organic acids

in permafrost fuel rapid carbon dioxide production upon thaw. *Proceedings of the National Academy of Sciences of the United States of America*, 112(45), 13946–13951. https://doi.org/10.1073/pnas.1511705112

Elder, C. D., Schweiger, M., Lam, B., Crook, E. D., Xu, X., Walker, J., Anthony, K. M. W., & Czimczik, C. I. (2019). Seasonal sources of whole-lake CH_4 and CO_2 emissions from Interior Alaskan thermokarst lakes. *Journal of Geophysical Research: Biogeosciences*, 124(5), 1209–1229. https://doi.org/10.1029/2018JG004735

Estop-Aragonés, C., Czimczik, C. I., Heffernan, L., Gibson, C., Walker, J. C., Xu, X., & Olefeldt, D. (2018). Respiration of aged soil carbon during fall in permafrost peatlands enhanced by active layer deepening following wildfire but limited following thermokarst. *Environmental Research Letters*, 13(8), 085002. https://doi.org/10.1088/1748-9326/aad5f0

Estop-Aragonés, C., Olefeldt, D., Abbott, B. W., Chanton, J. P., Czimczik, C. I., Dean, J. F., Egan, J. E., Gandois, L., Garnett, M. H., Hartley, I. P., Hoyt, A., Lupascu, M., Natali, S. M., O'Donnell, J. A., Raymond, P. A., Tanentzap, A. J., Tank, S. E., Schuur, E. A. G., Turetsky, M., & Anthony, K. W. (2020). Assessing the potential for mobilization of old soil carbon after permafrost thaw: A synthesis of ^{14}C measurements from the northern permafrost region. *Global Biogeochemical Cycles*, 34(9), e2020GB006672. https://doi.org/10.1029/2020GB006672

Evans, C. D., Page, S. E., Jones, T., Moore, S., Gauci, V., Laiho, R., Hruška, J., Allott, T. E. H., Billett, M. F., Tipping, E., Freeman, C., & Garnett, M. H. (2014). Contrasting vulnerability of drained tropical and high-latitude peatlands to fluvial loss of stored carbon. *Global Biogeochemical Cycles*, 28(11), 1215–1234. https://doi.org/10.1002/2013GB004782

Frey, K. E., & McClelland, J. W. (2009). Impacts of permafrost degradation on arctic river biogeochemistry. *Hydrological Processes*, 23(1), 169–182. https://doi.org/10.1002/hyp.7196

Frey, K. E., & Smith, L. C. (2005). Amplified carbon release from vast West Siberian peatlands by 2100. *Geophysical Research Letters*, 32(9). https://doi.org/10.1029/2004GL022025

Gandois, L., Hoyt, A. M., Hatté, C., Jeanneau, L., Teisserenc, R., Liotaud, M., & Tananaev, N. (2019). Contribution of peatland permafrost to dissolved organic matter along a thaw gradient in North Siberia. *Environmental Science & Technology*, 53(24), 14165–14174. https://doi.org/10.1021/acs.est.9b03735

Gibson, C. M., Chasmer, L. E., Thompson, D. K., Quinton, W. L., Flannigan, M. D., & Olefeldt, D. (2018). Wildfire as a major driver of recent permafrost thaw in boreal peatlands. *Nature Communications*, 9(1), 3041. https://doi.org/10.1038/s41467-018-05457-1

Gibson, J. J., Yi, Y., & Birks, S. J. (2019). Isotopic tracing of hydrologic drivers including permafrost thaw status for lakes across Northeastern Alberta, Canada: A 16-year, 50-lake assessment. *Journal of Hydrology*, 26, 100643. https://doi.org/10.1016/j.ejrh.2019.100643

Granath, G., Evans, C. D., Strengbom, J., Fölster, J., Grelle, A., Strömqvist, J., & Köhler, S. J. (2020). The impact of wildfire on biogeochemical fluxes and water quality on boreal catchments. *Biogeosciences Discussions*, 1–33, https://doi.org/10.5194/bg-2020-363

Grey, J. (2016). The incredible lightness of being methane-fuelled: Stable isotopes reveal alternative energy pathways in aquatic ecosystems and beyond. *Frontiers in Ecology and Evolution*, 4. https://doi.org/10.3389/fevo.2016.00008

Guillemette, F., Bianchi, T. S., & Spencer, R. G. M. (2017). Old before your time: Ancient carbon incorporation in contemporary aquatic food-webs. *Limnology and Oceanography*, 62(4), 1682–1700. https://doi.org/10.1002/lno.10525

Haynes, K. M., Connon, R. F., & Quinton, W. L. (2018). Permafrost thaw induced drying of wetlands at Scotty Creek, NWT, Canada. *Environmental Research Letters*, 13(11), 114001. https://doi.org/10.1088/1748-9326/aae46c

Heffernan, L., Estop-Aragonés, C., Knorr, K.-H., Talbot, J., & Olefeldt, D. (2020). Long-term impacts of permafrost thaw on carbon storage in peatlands: Deep losses offset by surficial accumulation. *Journal of Geophysical Research: Biogeosciences*, 125(3), e2019JG005501. https://doi.org/10.1029/2019JG005501

Helbig, M., Waddington, J. M., Alekseychik, P., Amiro, B. D., Aurela, M., Barr, A. G., Black, T. A., Blanken, P. D., Carey, S. K., Chen, J., Chi, J., Desai, A. R., Dunn, A., Euskirchen, E. S., Flanagan, L. B., Forbrich, I., Friborg, T., Grelle, A., Harder, S., … Zyrianov, V. (2020). Increasing contribution of peatlands to boreal evapotranspiration in a warming climate. *Nature Climate Change*, 10(6), 555–560. https://doi.org/10.1038/s41558-020-0763-7

Hoag, R. S., & Price, J. S. (1995). A field-scale, natural gradient solute transport experiment in peat at a Newfoundland blanket bog. *Journal of Hydrology*, 172(1), 171–184. https://doi.org/10.1016/0022-1694(95)02696-M

Holden, J., & Burt, T. P. (2003). Hydraulic conductivity in upland blanket peat: Measurement and variability. *Hydrological Processes*, 17(6), 1227–1237. https://doi.org/10.1002/hyp.1182

Hua, Q., Barbetti, M., & Rakowski, A. Z. (2013). Atmospheric radiocarbon for the period 1950–2010. *Radiocarbon*, 55(4), 2059–2072. https://doi.org/10.2458/azu_js_rc.v55i2.16177

Hugelius, G., Loisel, J., Chadburn, S., Jackson, R. B., Jones, M., MacDonald, G., Marushchak, M., Olefeldt, D., Packalen, M., Siewert, M. B., Treat, C., Turetsky, M., Voigt, C., & Yu, Z. (2020). Large stocks of peatland carbon and nitrogen are vulnerable to permafrost thaw. *Proceedings of the National Academy of Sciences of the United States of America*, 117(34), 20438–20446. https://doi.org/10.1073/pnas.1916387117

Hutchins, R. H. S., Tank, S. E., Olefeldt, D., Quinton, W. L., Spence, C., Dion, N., Estop-Aragonés, C., & Mengistu, S. G. (2020). Fluvial CO_2 and CH_4 patterns across wildfire-disturbed ecozones of subarctic Canada: Current status and implications for future change. *Global Change Biology*, 26(4), 2304–2319. https://doi.org/10.1111/gcb.14960

Ise, T., Dunn, A. L., Wofsy, S. C., & Moorcroft, P. R. (2008). High sensitivity of peat decomposition to climate change through water-table feedback. *Nature Geoscience*, 1(11), 763–766. https://doi.org/10.1038/ngeo331

Kankaala, P., Taipale, S., Grey, J., Sonninen, E., Arvola, L., & Jones, R. I. (2006). Experimental d13C evidence for a contribution of methane to pelagic food webs in lakes. *Limnology and Oceanography*, 51(6), 2821–2827. https://doi.org/10.4319/lo.2006.51.6.2821

Kawahigashi, M., Kaiser, K., Kalbitz, K., Rodionov, A., & Guggenberger, G. (2004). Dissolved organic matter in small streams along a gradient from discontinuous to continuous permafrost. *Global Change Biology*, 10(9), 1576–1586. https://doi.org/10.1111/j.1365-2486.2004.00827.x

Keeling, C. D., Piper, S. C., Bacastow, R. B., Wahlen, M., Whorf, T. P., Heimann, M., & Meijer, H. A. (2005). Atmospheric CO_2 and [13]CO_2 Exchange with the terrestrial biosphere and oceans from 1978 to 2000: observations and carbon cycle implications. In I. T. Baldwin, M. M. Caldwell, G. Heldmaier, R. B. Jackson, O. L. Lange, H. A. Mooney, E.-D. Schulze, U. Sommer, J. R. Ehleringer, M. Denise Dearing, & T. E. Cerling (Eds.), *A history of atmospheric CO_2 and its effects on plants, animals, and ecosystems* (pp. 83–113). Springer. https://doi.org/10.1007/0-387-27048-5_5

Kohzu, A., Kato, C., Iwata, T., Kishi, D., Murakami, M., Nakano, S., & Wada, E. (2004). Stream food web fueled by methane-derived carbon. *Aquatic Microbial Ecology*, 36(2), 189–194. https://doi.org/10.3354/ame036189

Kothawala, D. N., Kellerman, A. M., Catalán, N., & Tranvik, L. J. (2021). Organic matter degradation across ecosystem boundaries: The need for a unified conceptualization. *Trends in Ecology & Evolution*, 36(2), 113–122. https://doi.org/10.1016/j.tree.2020.10.006

Krüger, J. P., Leifeld, J., & Alewell, C. (2014). Degradation changes stable carbon isotope depth profiles in palsa peatlands. *Biogeosciences*, 11(12), 3369–3380. https://doi.org/10.5194/bg-11-3369-2014

Kuhry, P., & Turunen, J. (2006). The postglacial development of boreal and subarctic peatlands. In R. K. Wieder & D. H. Vitt (Eds.),

Boreal peatland ecosystems (pp. 25–46). Springer. https://doi.org/10.1007/978-3-540-31913-9_3

Lee, H., Schuur, E. A. G., Inglett, K. S., Lavoie, M., & Chanton, J. P. (2012). The rate of permafrost carbon release under aerobic and anaerobic conditions and its potential effects on climate. *Global Change Biology*, *18*(2), 515–527. https://doi.org/10.1111/j.1365-2486.2011.02519.x

Lehmann, J., Hansel, C. M., Kaiser, C., Kleber, M., Maher, K., Manzoni, S., Nunan, N., Reichstein, M., Schimel, J. P., Torn, M. S., Wieder, W. R., & Kögel-Knabner, I. (2020). Persistence of soil organic carbon caused by functional complexity. *Nature Geoscience*, *13*(8), 529–534. https://doi.org/10.1038/s41561-020-0612-3

Lehmann, J., & Kleber, M. (2015). The contentious nature of soil organic matter. *Nature*, *528*(7580), 60–68. https://doi.org/10.1038/nature16069

Leifeld, J., Steffens, M., & Galego-Sala, A. (2012). Sensitivity of peatland carbon loss to organic matter quality. *Geophysical Research Letters*, *39*(14). https://doi.org/10.1029/2012GL051856

Lennon, J. T., Faiia, A. M., Feng, X., & Cottingham, K. L. (2006). Relative importance of CO_2 recycling and CH_4 pathways in lake food webs along a dissolved organic carbon gradient. *Limnology and Oceanography*, *51*(4), 1602–1613. https://doi.org/10.4319/lo.2006.51.4.1602

Limpens, J., Berendse, F., Blodau, C., Canadell, J. G., Freeman, C., Holden, J., Roulet, N., Rydin, H., & Schaepman-Strub, G. (2008). Peatlands and the carbon cycle: From local processes to global implications – A synthesis. *Biogeosciences*, *5*(5), 1475–1491. https://doi.org/10.5194/bg-5-1475-2008

Littlefair, C. A., & Tank, S. E. (2018). Biodegradability of thermokarst carbon in a till-associated, glacial margin landscape: The case of the Peel Plateau, NWT, Canada. *Journal of Geophysical Research: Biogeosciences*, *123*(10), 3293–3307. https://doi.org/10.1029/2018JG004461

Loisel, J., Yu, Z., Beilman, D. W., Camill, P., Alm, J., Amesbury, M. J., Anderson, D., Andersson, S., Bochicchio, C., Barber, K., Belyea, L. R., Bunbury, J., Chambers, F. M., Charman, D. J., De Vleeschouwer, F., Fiałkiewicz-Kozieł, B., Finkelstein, S. A., Gałka, M., Garneau, M., … Zhou, W. (2014). A database and synthesis of northern peatland soil properties and Holocene carbon and nitrogen accumulation. *The Holocene*, *24*, 1028–1042. https://doi.org/10.1177/0959683614538073

Lynch, L. M., Machmuller, M. B., Boot, C. M., Covino, T. P., Rithner, C. D., Cotrufo, M. F., Hoyt, D. W., & Wallenstein, M. D. (2019). Dissolved organic matter chemistry and transport along an Arctic tundra hillslope. *Global Biogeochemical Cycles*, *33*(1), 47–62. https://doi.org/10.1029/2018GB006030

MacDonald, E. N., Tank, S. E., Kokelj, S. V., Froese, D. G., & Hutchins, R. H. S. (2021). Permafrost-derived dissolved organic matter composition varies across permafrost end-members in the western Canadian Arctic. *Environmental Research Letters*, *16*(2), 024036. https://doi.org/10.1088/1748-9326/abd971

Mann, P. J., Eglinton, T. I., McIntyre, C. P., Zimov, N., Davydova, A., Vonk, J. E., Holmes, R. M., & Spencer, R. G. M. (2015). Utilization of ancient permafrost carbon in headwaters of Arctic fluvial networks. *Nature Communications*, *6*(1), 7856. https://doi.org/10.1038/ncomms8856

Moore, S., Evans, C. D., Page, S. E., Garnett, M. H., Jones, T. G., Freeman, C., Hooijer, A., Wiltshire, A. J., Limin, S. H., & Gauci, V. (2013). Deep instability of deforested tropical peatlands revealed by fluvial organic carbon fluxes. *Nature*, *493*(7434), 660–663. https://doi.org/10.1038/nature11818

Neff, J. C., Finlay, J. C., Zimov, S. A., Davydov, S. P., Carrasco, J. J., Schuur, E. A. G., & Davydova, A. I. (2006). Seasonal changes in the age and structure of dissolved organic carbon in Siberian rivers and streams. *Geophysical Research Letters*, *33*(23). https://doi.org/10.1029/2006GL028222

Nykänen, H., Peura, S., Kankaala, P., & Jones, R. I. (2014). Recycling and fluxes of carbon gases in a stratified boreal lake following experimental carbon addition. *Biogeosciences Discussions*, *11*(11), 16447–16495. https://doi.org/10.5194/bgd-11-16447-2014

O'Donnell, J. A., Aiken, G. R., Walvoord, M. A., Raymond, P. A., Butler, K. D., Dornblaser, M. M., & Heckman, K. (2014). Using dissolved organic matter age and composition to detect permafrost thaw in boreal watersheds of interior Alaska. *Journal of Geophysical Research: Biogeosciences*, *119*(11), 2155–2170. https://doi.org/10.1002/2014JG002695

O'Donnell, J. A., Carey, M. P., Koch, J. C., Xu, X., Poulin, B. A., Walker, J., & Zimmerman, C. E. (2020). Permafrost hydrology drives the assimilation of old carbon by stream food webs in the Arctic. *Ecosystems*, *23*(2), 435–453. https://doi.org/10.1007/s10021-019-00413-6

O'Donnell, J. A., Jorgenson, M. T., Harden, J. W., McGuire, A. D., Kanevskiy, M. Z., & Wickland, K. P. (2012). The effects of permafrost thaw on soil hydrologic, thermal, and carbon dynamics in an Alaskan peatland. *Ecosystems*, *15*(2), 213–229. https://doi.org/10.1007/s10021-011-9504-0

Olefeldt, D., Euskirchen, E. S., Harden, J., Kane, E., McGuire, A. D., Waldrop, M. P., & Turetsky, M. R. (2017). A decade of boreal rich fen greenhouse gas fluxes in response to natural and experimental water table variability. *Global Change Biology*, *23*(6), 2428–2440. https://doi.org/10.1111/gcb.13612

Olefeldt, D., Goswami, S., Grosse, G., Hayes, D., Hugelius, G., Kuhry, P., McGuire, A. D., Romanovsky, V. E., Sannel, A. B. K., Schuur, E. A. G., & Turetsky, M. R. (2016). Circumpolar distribution and carbon storage of thermokarst landscapes. *Nature Communications*, *7*(1), 13043. https://doi.org/10.1038/ncomms13043

Olefeldt, D., Persson, A., & Turetsky, M. R. (2014). Influence of the permafrost boundary on dissolved organic matter characteristics in rivers within the Boreal and Taiga plains of western Canada. *Environmental Research Letters*, *9*(3), 035005. https://doi.org/10.1088/1748-9326/9/3/035005

Olefeldt, D., Turetsky, M. R., Crill, P. M., & McGuire, A. D. (2013). Environmental and physical controls on northern terrestrial methane emissions across permafrost zones. *Global Change Biology*, *19*(2), 589–603. https://doi.org/10.1111/gcb.12071

Olid, C., Zannella, A., & Lau, D. C. P. (2021). The role of methane transport from the active layer in sustaining methane emissions and food chains in subarctic ponds. *Journal of Geophysical Research: Biogeosciences*, *126*(3), e2020JG005810. https://doi.org/10.1029/2020JG005810

Pelletier, N., Talbot, J., Olefeldt, D., Turetsky, M., Blodau, C., Sonnentag, O., & Quinton, W. L. (2017). Influence of Holocene permafrost aggradation and thaw on the paleoecology and carbon storage of a peatland complex in northwestern Canada. *The Holocene*, *27*(9), 1391–1405. https://doi.org/10.1177/0959683617693899

Perryman, C. R., McCalley, C. K., Malhotra, A., Fahnestock, M. F., Kashi, N. N., Bryce, J. G., Giesler, R., & Varner, R. K. (2020). Thaw transitions and redox conditions drive methane oxidation in a permafrost peatland. *Journal of Geophysical Research: Biogeosciences*, *125*(3), e2019JG005526. https://doi.org/10.1029/2019JG005526

Persaud, A. D., Dillon, P. J., Lasenby, D., & Yan, N. D. (2009). Stable isotope variability of meso-zooplankton along a gradient of dissolved organic carbon. *Freshwater Biology*, *54*(8), 1705–1719. https://doi.org/10.1111/j.1365-2427.2009.02224.x

Pinsonneault, A. J., Moore, T. R., Roulet, N. T., & Lapierre, J.-F. (2016). Biodegradability of vegetation-derived dissolved organic carbon in a cool temperate ombrotrophic bog. *Ecosystems*, *19*(6), 1023–1036. https://doi.org/10.1007/s10021-016-9984-z

Prėskienis, V., Laurion, I., Bouchard, F., Douglas, P. M. J., Billett, M. F., Fortier, D., & Xu, X. (2021). Seasonal patterns in greenhouse gas emissions from lakes and ponds in a High Arctic polygonal landscape. *Limnology and Oceanography*, *66*(S1), S117–S141. https://doi.org/10.1002/lno.11660

Quinton, W. L., & Baltzer, J. L. (2013). The active-layer hydrology of a peat plateau with thawing permafrost (Scotty Creek, Canada). *Hydrogeology Journal*, *21*(1), 201–220. https://doi.org/10.1007/s10040-012-0935-2

Quinton, W., Berg, A., Braverman, M., Carpino, O., Chasmer, L., Connon, R., Craig, J., Devoie, É., Hayashi, M., Haynes, K., Olefeldt, D., Pietroniro, A., Rezanezhad, F., Schincariol, R., & Sonnentag, O. (2019). A synthesis of three decades of hydrological research at Scotty Creek, NWT, Canada. *Hydrology and Earth System Sciences*, 23(4), 2015–2039. https://doi.org/10.5194/hess-23-2015-2019

Raghoebarsing, A. A., Smolders, A. J. P., Schmid, M. C., Rijpstra, W. I. C., Wolters-Arts, M., Derksen, J., Jetten, M. S. M., Schouten, S., Sinninghe Damsté, J. S., Lamers, L. P. M., Roelofs, J. G. M., Op den Camp, H. J. M., & Strous, M. (2005). Methanotrophic symbionts provide carbon for photosynthesis in peat bogs. *Nature*, 436(7054), 1153–1156. https://doi.org/10.1038/nature03802

Raymond, P. A., McClelland, J. W., Holmes, R. M., Zhulidov, A. V., Mull, K., Peterson, B. J., Striegl, R. G., Aiken, G. R., & Gurtovaya, T. Y. (2007). Flux and age of dissolved organic carbon exported to the Arctic Ocean: A carbon isotopic study of the five largest arctic rivers. *Global Biogeochemical Cycles*, 21(4), GB4011. https://doi.org/10.1029/2007GB002934

Reimer, P. J., Baillie, M. G. L., Bard, E., Bayliss, A., Beck, J. W., Bertrand, C. J. H., Blackwell, P. G., Buck, C. E., Burr, G. S., Cutler, K. B., Damon, P. E., Edwards, R. L., Fairbanks, R. G., Friedrich, M., Guilderson, T. P., Hogg, A. G., Hughen, K. A., Kromer, B., McCormac, G., … Weyhenmeyer, C. E. (2004). IntCal04 terrestrial radiocarbon age calibration, 0–26 cal kyr BP. *Radiocarbon*, 46(3), 1029–1058.

Reimer, P. J., Bard, E., Bayliss, A., Beck, J. W., Blackwell, P. G., Ramsey, C. B., Buck, C. E., Cheng, H., Edwards, R. L., Friedrich, M., Grootes, P. M., Guilderson, T. P., Haflidason, H., Hajdas, I., Hatté, C., Heaton, T. J., Hoffmann, D. L., Hogg, A. G., Hughen, K. A., … van der Plicht, J. (2013). IntCal13 and Marine13 radiocarbon age calibration curves 0–50,000 years cal BP. *Radiocarbon*, 55(4), 1869–1887. https://doi.org/10.2458/azu_js_rc.55.16947

Schädel, C., Bader, M.-F., Schuur, E. A. G., Biasi, C., Bracho, R., Čapek, P., De Baets, S., Diáková, K., Ernakovich, J., Estop-Aragones, C., Graham, D. E., Hartley, I. P., Iversen, C. M., Kane, E., Knoblauch, C., Lupascu, M., Martikainen, P. J., Natali, S. M., Norby, R. J., … Wickland, K. P. (2016). Potential carbon emissions dominated by carbon dioxide from thawed permafrost soils. *Nature Climate Change*, 6(10), 950–953. https://doi.org/10.1038/nclimate3054

Schuur, E. A. G., McGuire, A. D., Schädel, C., Grosse, G., Harden, J. W., Hayes, D. J., Hugelius, G., Koven, C. D., Kuhry, P., Lawrence, D. M., Natali, S. M., Olefeldt, D., Romanovsky, V. E., Schaefer, K., Turetsky, M. R., Treat, C. C., & Vonk, J. E. (2015). Climate change and the permafrost carbon feedback. *Nature*, 520(7546), 171–179. https://doi.org/10.1038/nature14338

Seeberg-Elverfeldt, J., Schlüter, M., Feseker, T., & Kölling, M. (2005). Rhizon sampling of porewaters near the sediment-water interface of aquatic systems. *Limnology and Oceanography: Methods*, 3(8), 361–371. https://doi.org/10.4319/lom.2005.3.361

Selvam, B. P., Lapierre, J.-F., Guillemette, F., Voigt, C., Lamprecht, R. E., Biasi, C., Christensen, T. R., Martikainen, P. J., & Berggren, M. (2017). Degradation potentials of dissolved organic carbon (DOC) from thawed permafrost peat. *Scientific Reports*, 7(1), 45811. https://doi.org/10.1038/srep45811

Shur, Y. L., & Jorgenson, M. T. (2007). Patterns of permafrost formation and degradation in relation to climate and ecosystems. *Permafrost and Periglacial Processes*, 18(1), 7–19. https://doi.org/10.1002/ppp.582

Street, L. E., Dean, J. F., Billett, M. F., Baxter, R., Dinsmore, K. J., Lessels, J. S., Subke, J.-A., Tetzlaff, D., & Wookey, P. A. (2016). Redox dynamics in the active layer of an Arctic headwater catchment; examining the potential for transfer of dissolved methane from soils to stream water. *Journal of Geophysical Research: Biogeosciences*, 121(11), 2776–2792. https://doi.org/10.1002/2016JG003387

Tanentzap, A. J., Kielstra, B. W., Wilkinson, G. M., Berggren, M., Craig, N., del Giorgio, P. A., Grey, J., Gunn, J. M., Jones, S. E., Karlsson, J., Solomon, C. T., & Pace, M. L. (2017). Terrestrial support of lake food webs:

Synthesis reveals controls over cross-ecosystem resource use. *Science Advances*, 3(3), e1601765. https://doi.org/10.1126/sciadv.1601765

Turetsky, M. R., Wieder, R. K., Vitt, D. H., Evans, R. J., & Scott, K. D. (2007). The disappearance of relict permafrost in boreal North America: Effects on peatland carbon storage and fluxes. *Global Change Biology*, 13(9), 1922–1934. https://doi.org/10.1111/j.1365-2486.2007.01381.x

Vehtari, A., Gelman, A., & Gabry, J. (2017). Practical Bayesian model evaluation using leave-one-out cross-validation and WAIC. *Statistics and Computing*, 27(5), 1413–1432. https://doi.org/10.1007/s11222-016-9696-4

Vonk, J. E., Mann, P. J., Davydov, S., Davydova, A., Spencer, R. G. M., Schade, J., Sobczak, W. V., Zimov, N., Zimov, S., Bulygina, E., Eglinton, T. I., & Holmes, R. M. (2013). High biolability of ancient permafrost carbon upon thaw. *Geophysical Research Letters*, 40(11), 2689–2693. https://doi.org/10.1002/grl.50348

Vonk, J. E., Tank, S. E., Bowden, W. B., Laurion, I., Vincent, W. F., Alekseychik, P., Amyot, M., Billet, M. F., Canário, J., Cory, R. M., Deshpande, B. N., Helbig, M., Jammet, M., Karlsson, J., Larouche, J., MacMillan, G., Rautio, M., Walter Anthony, K. M., & Wickland, K. P. (2015). Reviews and syntheses: Effects of permafrost thaw on Arctic aquatic ecosystems. *Biogeosciences*, 12(23), 7129–7167. https://doi.org/10.5194/bg-12-7129-2015

Whiticar, M. J. (1996). Stable isotope geochemistry of coals, humic kerogens and related natural gases. *International Journal of Coal Geology*, 32(1), 191–215. https://doi.org/10.1016/S0166-5162(96)00042-0

Whiticar, M. J. (1999). Carbon and hydrogen isotope systematics of bacterial formation and oxidation of methane. *Chemical Geology*, 161(1), 291–314. https://doi.org/10.1016/S0009-2541(99)00092-3

Wigley, T. M. L., Plummer, L. N., & Pearson, F. J. (1978). Mass transfer and carbon isotope evolution in natural water systems. *Geochimica et Cosmochimica Acta*, 42(8), 1117–1139. https://doi.org/10.1016/0016-7037(78)90108-4

Wild, B., Andersson, A., Bröder, L., Vonk, J., Hugelius, G., McClelland, J. W., Song, W., Raymond, P. A., & Gustafsson, Ö. (2019). Rivers across the Siberian Arctic unearth the patterns of carbon release from thawing permafrost. *Proceedings of the National Academy of Sciences of the United States of America*, 116(21), 10280–10285. https://doi.org/10.1073/pnas.1811797116

Wilson, R. M., Hopple, A. M., Tfaily, M. M., Sebestyen, S. D., Schadt, C. W., Pfeifer-Meister, L., Medvedeff, C., McFarlane, K. J., Kostka, J. E., Kolton, M., Kolka, R. K., Kluber, L. A., Keller, J. K., Guilderson, T. P., Griffiths, N. A., Chanton, J. P., Bridgham, S. D., & Hanson, P. J. (2016). Stability of peatland carbon to rising temperatures. *Nature Communications*, 7(1), 13723. https://doi.org/10.1038/ncomms13723

Wright, N., Hayashi, M., & Quinton, W. L. (2009). Spatial and temporal variations in active layer thawing and their implication on runoff generation in peat-covered permafrost terrain. *Water Resources Research*, 45(5). https://doi.org/10.1029/2008WR006880.

Yao, Y., Vehtari, A., Simpson, D., & Gelman, A. (2018). Using stacking to average Bayesian predictive distributions (with discussion). *Bayesian Analysis*, 13(3), 917–1007. https://doi.org/10.1214/17-BA1091

SUPPORTING INFORMATION

Additional supporting information may be found online in the Supporting Information section.

How to cite this article: Tanentzap, A. J., Burd, K., Kuhn, M., Estop-Aragonés, C., Tank, S. E., & Olefeldt, D. (2021). Aged soils contribute little to contemporary carbon cycling downstream of thawing permafrost peatlands. *Global Change Biology*, 00, 1–15. https://doi.org/10.1111/gcb.15756